Original Article
The human positive cofactor 4 promotes androgen-independent prostate cancer development and progression through HIF-1α/β-catenin pathway

Peng Luo[1], Qingzhi Jiang[1,4], Qiang Fang[2], Yawei Wang[1], Ziwen Wang[1], Jing Yang[3], Xu Tan[1], Weibing Li[2], Chunmeng Shi[1]

[1]Institute of Rocket Force Medicine, State Key Laboratory of Trauma, Burns and Combined Injury, Third Military Medical University, Chongqing 400038, China; [2]Department of Urology and Nephrology, The Third Affiliated Hospital of Chongqing Medical University, Chongqing 401120, China; [3]Institute of Pathology and Southwest Cancer Center, Southwest Hospital, Third Military Medical University, Chongqing 400038, China; [4]Institute of Clinical Medicine, Southwest Medical University, Luzhou 646000, Sichuan, China

Abstract: Androgen-dependent prostate cancer (ADPC) eventually progresses to androgen-independent prostate cancer (AIPC), that has a poor prognosis owing to its unclear mechanism and lack of effective therapeutic targets. The human positive cofactor 4 (PC4) is a transcriptional cofactor, and plays a potential role in cancer development. However, the significance and mechanism of PC4 in AIPC progression are unclear. By analyzing the clinical data, we find that PC4 is overexpressed in prostate cancer and closely correlated with the progression, metastasis and prognosis of patients. Additionally, PC4 is significantly upregulated in AIPC cells compared with ADPC cells, implying its importance in the development and progression of AIPC. Then, in vivo and in vitro studies reveal that loss of PC4 inhibits cell growth by suppressing c-Myc/P21 pathway and inducing cell cycle arrest at G1/S phase transition in AIPC. PC4 knockdown also attenuates EMT-mediated metastasis in AIPC. Moreover, for the first time, we find that PC4 exerts its oncogenic functions by promoting the expression of HIF-1α and activating β-catenin signaling. Therefore, our findings determine the signatures and molecular mechanisms of PC4 in AIPC, and indicate that PC4 might be a promising therapeutic target for AIPC.

Keywords: Androgen-independent prostate cancer, positive cofactor 4, β-catenin, hypoxia-inducible factor-1α, proliferation, metastasis

Introduction

Prostate cancer is one of the most common malignant cancers and a leading cause of tumor-related death in males worldwide [1, 2]. In the early stage, prostate cancer patients are usually androgen-dependent prostate cancer (ADPC), and androgen deprivation therapy (ADT) is the mainstay of treatment [3, 4]. However, the majority of prostate cancer patients eventually progress to androgen-independent prostate cancer (AIPC), that is resistant to ADT and also known as castration-resistant prostate cancer (CRPC) [5]. Compared with ADPC, the incidence of local recurrence and distant metastasis in AIPC is markedly increased, and its prognosis is poor [6]. Thus, it is necessary to clarify the underlying molecular mechanisms of

AIPC progression and identify novel therapeutic targets to improve AIPC patients' outcomes [7].

Hypoxia is a common phenomenon in solid tumors including prostate cancer [8], and cellular response to hypoxia is mainly mediated by hypoxia-inducible factor-1α (HIF-1α) [9, 10]. As a nuclear transcription factor, HIF-1α binds to the hypoxia response elements of target genes and regulates various cellular processes including cell metabolism, growth, differentiation and angiogenesis [11, 12]. In clinical samples of prostate cancer, HIF-1α is found to be overexpressed and correlated with histologic grade, distant metastasis and prognosis of patients [13, 14]. Moreover, targeting HIF-1α can enhance the radiosensitivity in prostate cancer cells [15-17]. Although HIF-1α plays an

important role in prostate cancer progression and treatment response, the molecular mechanisms of HIF-1α in AIPC progression are unclear and remain to be elucidated [18, 19].

The human positive cofactor 4 (PC4) is a highly-conserved nuclear protein and initially identified as transcriptional cofactor, that facilitates RNA polymerase II-driven gene transcription [20-22]. PC4 is composed of 127 amino acid residues with a C-terminal DNA-binding domain and an N-terminal transcriptional co-activating domain [23-25]. Increasing evidences show that PC4 is involved in various molecular biological processes including basal transcription, DNA replication, DNA repair and chromatin organization [26-31]. Previous studies by our group and others have identified that upregulation of PC4 in several cancer types is involved in cancer development, lymphatic metastasis and radiosensitivity [24, 32-35]. However, the signatures and molecular mechanisms of PC4 in AIPC progression still need to be clarified.

In this study, we demonstrate that overexpression of PC4 in prostate cancer is closely correlated with progression, metastasis and poor prognosis of patients. Then, PC4 is significantly upregulated in AIPC cells compared with ADPC cells, suggesting its importance in AIPC progression. Apart from the decreased EMT-mediated metastasis, PC4 knockdown is also found to inhibit cell growth by suppressing c-Myc/P21-mediated G1/S transition in AIPC. Mechanistically, PC4 maintains its malignant phenotypes through HIF-1α/β-catenin pathway. Thus, PC4 plays an oncogenic role in AIPC and holds promise for cancer targeted therapy.

Materials and methods

Animals

Athymic male nude mice (4-6 weeks) were obtained from the Center for Experimental Animals in a specific pathogen-free condition. Animal experiments were followed the Guidelines for the Care and Use of Laboratory Animals of the TMMU, and all procedures were approved by the Animal Care and Use Committee of the TMMU.

Cell lines

The human prostate cancer cell lines (LAPC4, C4-2, PC3 and DU145) and non-cancerous

prostate epithelial cell lines (RWPE-1) were purchased from the American Type Culture Collection (ATCC, Manassas, Virginia, USA) and the Cell Bank of the Chinese (Shanghai, China). C4-2, PC3, DU145 were grown in RPMI-1640 (Hyclone, Logan, Utah, USA), LAPC4 was grown in DMEM (Hyclone, Logan, Utah, USA), and RWPE-1 was grown in K-SFM (Gibco, Grand Island New York, USA). All cells were cultured in the above medium, supplemented with 10% FBS (Gibco, Grand Island New York, USA) and 1% streptomycin/penicillin (Beyotime, Shanghai, China), and incubated in 5% CO_2 at 37°C.

Clinical samples

The prostate cancer samples and paired adjacent normal tissues were collected from Southwest Hospital of Third Military Medical University. All prostate cancer patients were diagnosed independently by at least two experienced pathologists, according to the Union for International Cancer Control classification system. This study was approved by the Ethics Committee of Third Military Medical University.

RNA interference and in vitro overexpression

The shRNA lentivirus vector targeting human PC4 (shRNA: 5'-ACAGAGCAGCAGCAGCAGATT-3'; 5'-UCUGCUGCUGCUGCUCUGUTT-3') and negative control shRNA (5'-UUCUCCGAACGUGU-CACGUTT-3'; 5'-ACGUGACACGUUCGGAGAATT-3') were constructed by GeneChem (Shanghai, China). The human HIF-1α plasmid were purchased from GeneChem (Shanghai, China). The human β-catenin plasmid was purchased from Fenghbio (Hunan, China). According to the manufacturer's protocol, PC3 and DU145 cells were transfected with plasmid using Lipofectamine 3000 (Invitrogen) in OptiMEM (Hyclone) according to the manufactures' instructions.

Cell viability assay and colony formation assay

Cell viability assay was measured by the Cell Counting Kit-8 (Dojindo, Kumamoto, Japan). Briefly, the PC3 or DU145 cells with stable PC4 knockdown and controls were seeded into 96-well plates (3000 cells per well with 100 ul medium) and cultured in 5% CO_2 incubator at 37°C. Cell viability was tested at 24 h, 48 h, 72 h and 96 at a wavelength of 450 nm (OD450). Experiments were performed in triplicate. For colony formation assay, the PC3 or DU145 cells

with stable PC4 knockdown and controls were trypsinized and seeded in 6-well plates. The medium was changed every three days, and cells were cultured for 14 d-21 d until colonies were clearly visible. At the endpoint, cells were washed twice with PBS, fixed with 4% paraformaldehyde, stained with crystal violet (Beyotime, China) for 30 minutes, and then colonies with > 50 cells were counted. Experiments were performed in triplicate.

Scratch-wound assay and transwell assay

For scratch-wound assay, the PC3 or DU145 cells with stable PC4 knockdown and controls were seeded into 6-well plates. When they grew to full confluence, wounds were generated in the monolayer cells by a 10 ul pipette tip and dead cells were washed by PBS. Then, cells were cultured in serum-free medium and photographed at the indicated time. Experiments were performed in triplicate. For transwell assay, cells were suspended in serum-free medium and seeded into the upper chamber of the transwell (8 μm, Corning, NY, USA) with Matrigel (BD Pharmingen). The lower chamber was filled with culture medium containing 10% FBS. After incubation for 24 h, cells were removed from the upper chamber, and the bottom of the filter were fixed in paraformaldehyde for 15 mins and stained with crystal violet. Under microscopy, cells were counted from five different fields of inserts. Experiments were performed in triplicate.

Cell cycle and apoptosis analysis by flow cytometry

For analysis of cell cycle distribution, the PC3 or DU145 cells with stable PC4 knockdown and controls were collected and fixed using 75% ethanol at -20°C overnight. After incubating with propidium iodide (PI, 50 μg/mL) and RNase for 20 min at 37°C in the dark, cells were analyzed by flow cytometry. For apoptosis analysis, cells were stained with AnnexinV-FITC/PI (BD Biosciences) for 15 min at 37°C in the dark, and then analyzed by flow cytometry. Experiments were performed in triplicate.

Quantitative real-time PCR

Total RNA in PC3 or DU145 cells were extracted using Trizol reagent (Invitrogen, CA, USA). According to the manufacturer's instruction,

Real-time PCR was performed using a SYBR Green kit (Takara). The primers for PC4, HIF-1α and β-actin are listed in Table S1.

Western blot analysis

Total proteins in PC3 or DU145 cells were extracted using RIPA buffer (Beyotime) and quantitated by a BCA kit (Beyotime). The protein samples were separated by electrophoresis, transferred to PVDF membranes (Millipore), and incubated with primary antibodies overnight at 4°C. After washing and incubating 1 hour with HRP-linked secondary antibody (Cell Signaling Technology, USA) at room temperature, the membranes were visualized and detected by an enhanced chemiluminescence detection system (Bio-Rad Laboratories). Primary antibodies against c-Myc, P21, Cyclin D, Cyclin E, CDK6, Rb, PRb (ser807/811), PARP, Pro-Caspase 3, Cleaved-Caspase 3, Snail, E-cadherin, N-cadherin and β-catenin were obtained from Cell Signaling Technology. Primary antibodies against HIF-1α were obtained from Abcam. Primary antibodies against PC4 were obtained from Sigma, Primary antibodies against β-actin were obtained from Santa Cruz Biotechnology.

Immunohistochemical staining

Immunohistochemical Staining was performed as previously described. After dewaxing, rehydrating, antigen retrieval and blocking nonspecific binding, the paraffin-embedded sections of prostate cancer tissues and adjacent normal tissues were incubated with primary PC4 antibody (1:500, Sigma) at 4°C overnight. Then, the slides were sequentially incubated with biotinylated secondary antibody and visualized by using DAB. Positive PC4 expression in prostate cancer is located in the nucleus. All tissue samples were examined and independently evaluated by two pathologists.

In vivo tumor growth and metastasis model

For in vivo tumor growth model, 100 ul PBS containing 5×10^6 PC4 stable knockdown PC3 cells or controls were injected subcutaneously at one dorsal site of athymic male nude mice. Tumor growth was measured every 2 days, and tumor volume was calculated by the following formula: volume (mm^3) = (width^2 × length)/2. At the endpoint, the mice were sacrificed, and

xenografts were dissected, weighed and fixed in 4% paraformaldehyde for next immunohisto-chemical staining.

For in vivo metastasis model, PC4 stable knock-down PC3 cells and controls (1 × 10⁶) were suspended in 200 ul PBS and injected into the tail vein of athymic male nude mice. At the end-point, the mice were sacrificed, and the lung tissues were fixed in 4% paraformaldehyde for next hematoxylin-eosin (HE) staining.

Statistical analysis

All data are presented as means ± SD. The statistical analysis was carried out using SPSS 13.0 software (SPSS Inc., Chicago, USA). Comparisons between two groups were performed using the Student's t-test. Comparisons among three or more groups were performed using a one-way analysis of variance (ANOVA). The survival data was performed using the Kaplan-Meier method. Correlation between PC4 expression and clinical parameters was determined using the Pearson's χ^2 method. P<0.05 was considered to be statistically significant.

Results

Overexpression of PC4 in prostate cancer is closely correlated with progression, metastasis and poor prognosis of patients

To investigate the role of PC4 in the development and progression of prostate cancer, we firstly analyzed PC4 expression level in prostate cancer specimens compared with their adjacent normal tissue. As shown in **Figure 1A**, high levels of PC4 were detected in carcinoma tissues, while almost undetectable levels in adjacent normal tissue. The average staining score of PC4 expression confirmed above results (**Figure 1B**), implying a potential role of PC4 in tumorigenesis. Then, we evaluated the possible correlation between PC4 expression and differentiation grade, and found that the intensity of PC4 in poorly differentiated tissue was significantly increased compared with that in well differentiated tissue (**Figure 1C** and **1D**). Moreover, PC4 expression in carcinoma with metastasis was obviously upregulated than that without metastasis (**Figure 1E** and **1F**). Finally, through analyzing 281 cases of prostate cancer from public cancer databases

(GSE16560), we found that the higher PC4 expression group had poorer overall survival compared with lower PC4 expression group (**Figure 1G** and **1H**). Collectively, these results suggest that PC4 is a potential oncogene and prognostic marker in prostate cancer.

PC4 is significantly upregulated in androgen-independent prostate cancer cells

To further validate the overexpression of PC4 in prostate cancer, we extended the analysis to in vitro cell culture models. The qPCR (**Figure 2A**) and Western blot (**Figure 2B**) assays confirmed that the mRNA and protein level of PC4 were upregulated in prostate cancer cell lines (LAPC4, C4-2, PC3 and DU145) compared with non-cancerous prostate epithelial cell lines (RWPE-1). Moreover, the expression of PC4 was significantly elevated in AIPC cell lines (C4-2, PC3 and DU145) than that in ADPC cell lines (LAPC4). To our knowledge, AIPC cells have a more aggressive and invasive phenotype. Immunofluorescent staining (**Figure 2C**) for PC4 revealed prominent nuclear localization, and exhibited high signal intensity in C4-2, PC3 and DU145 cells, medium signal intensity in LAPC4 cells, and low signal intensity in benign RWPE-1 cells. Taken together, these results exhibit that PC4 is significantly upregulated in AIPC cells, suggesting its importance in the development and progression of AIPC.

Silencing of PC4 inhibits androgen-independent prostate cancer cell growth both in vitro and in vivo

To investigate the functional significance of increased PC4 expression in AIPC, PC3 and DU145 cells were chosen for subsequent loss-of-function study. The stable cell lines with PC4 knockdown were established by specific shRNA (**Figures 3A** and S1). The cell viability and colony formation assays demonstrated that PC4 knockdown inhibited the proliferation (**Figure 3B**) and colony formation capacity (**Figure 3C** and **3D**) of AIPC cells. In addition, we established a subcutaneous xenograft model to determine the biological function of PC4 in vivo. PC3 cells with stable PC4-knockdown were inoculated into athymic male nude mice. During the whole experiment, xenograft growth in the sh-PC4 group was dramatically attenuated compared with the control groups (**Figure 3E**). The average tumor size and tumor weight at the
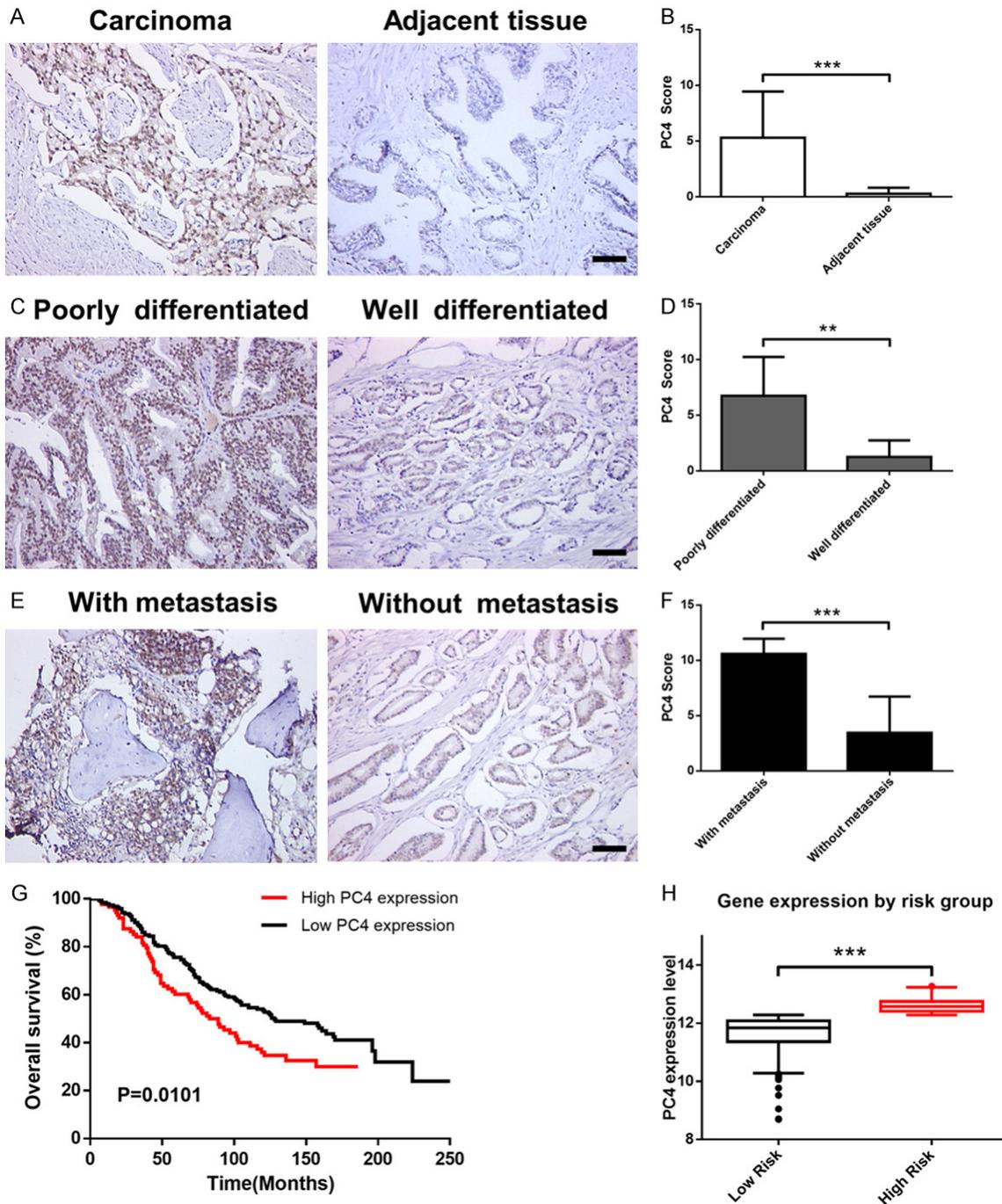
Figure 1. Overexpression of PC4 in prostate cancer is closely correlated with progression, metastasis and poor prognosis of patients. (A) Immunohistochemical staining for PC4 protein in prostate cancer tissues and their adjacent normal tissue. Scale bar represents 50 μm. (B) The average staining score of PC4 expression in prostate cancer derived from (A). (C) Immunohistochemical staining for PC4 protein in various differentiation degrees of human prostate cancer samples. Scale bar represents 50 μm. (D) The average staining score of PC4 expression in prostate cancer derived from (C). (E) Immunohistochemical staining for PC4 protein in prostate cancer tissues with or without metastasis. Scale bar represents 50 μm. (F) The average staining score of PC4 expression in prostate cancer derived from (E). (G) Kaplan-Meier analysis of the correlation between PC4 expression levels and overall survival in prostate cancer (n = 281). Data was obtained from GSE16560. (H) PC4 expression levels stratified by risk group. All data indicate the mean ± SD. **P<0.01, ***P<0.001.

experimental endpoint was inhibited by PC4 knockdown (**Figure 3F** and **3G**). Furthermore,

we detected the expressions of Ki67 as markers of proliferation. Consistently, sh-PC4 group
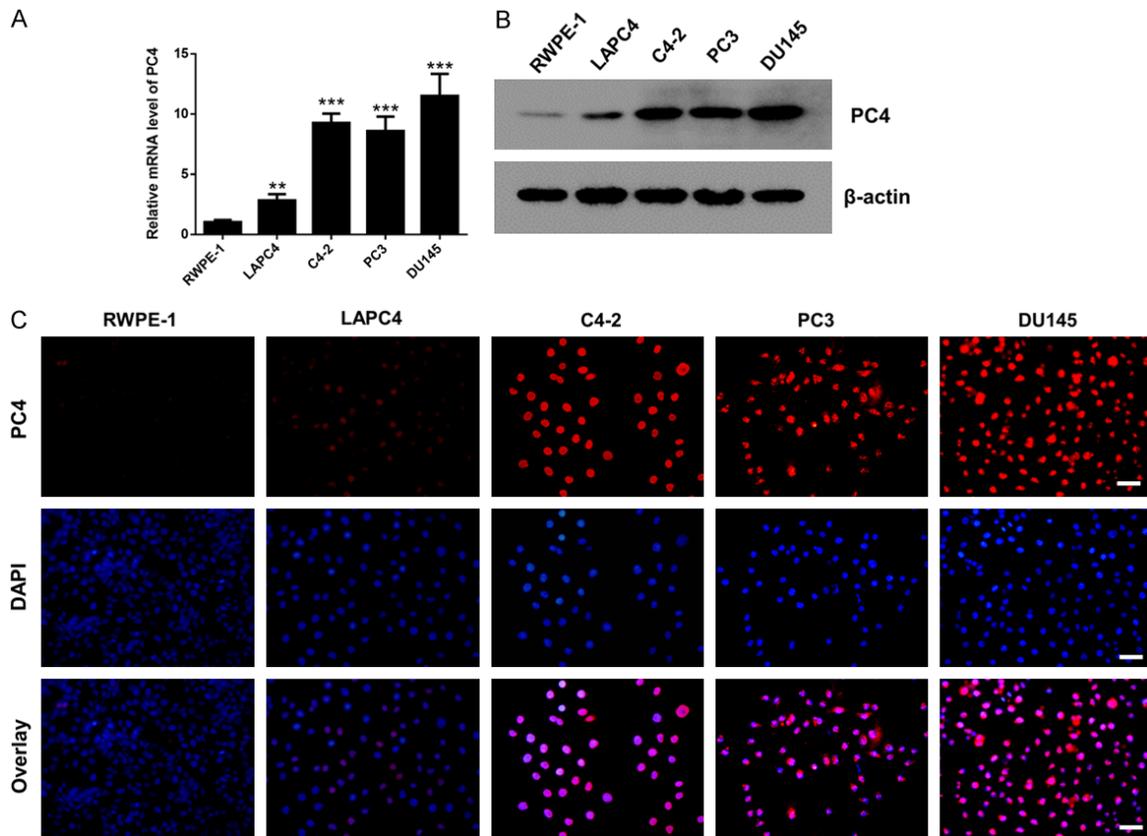
Figure 2. PC4 is significantly upregulated in androgen-independent prostate cancer cells. A. The mRNA level of PC4 in non-cancerous prostate epithelial cell lines (RWPE-1) and prostate cancer cell lines (LAPC4, C4-2, PC3 and DU145). LAPC4 is ADPC cell lines, C4-2, PC3 and DU145 are AIPC cell lines. B. The protein level of PC4 in non-cancerous prostate epithelial cell lines (RWPE-1) and prostate cancer cell lines (LAPC4, C4-2, PC3 and DU145). C. Immunofluorescent staining for PC4 expression in non-cancerous prostate epithelial cell lines (RWPE-1) and prostate cancer cell lines (LAPC4, C4-2, PC3 and DU145). Scale bar represents 50 μm. All data indicate the mean ± SD. **P<0.01, ***P<0.001.

presented a status of proliferation inhibition compared with the control groups (**Figure 3H** and **3I**). These results indicate that PC4 promotes AIPC cell growth both in vitro and in vivo.

Loss of PC4 induces cell cycle arrest at the G1-to-S phase transition through inhibiting c-Myc/P21 pathway

In search for the potential mechanism of PC4 on cell growth inhibition, the cell cycle distribution was determined by flow cytometry. As shown in **Figure 4A** and **4B**, silencing of PC4 caused more cells to arrest in the G1 phase and fewer cells entering the S phase, which mean G1/S phase arrest. Besides, knockdown of PC4 had no significant impact on cell apoptosis in both PC3 and DU145 cells (**Figures 4C**, **4D** and S2). To further investigate how PC4 regulates G1/S phase transition, we detected

the expression of cell cycle related proteins. As shown in **Figure 4E**, depletion of PC4 led to an increased expression of p21 and decreased expression of c-Myc, Cyclin D, Cyclin E and CDK6. Correspondingly, we found the steady-state levels of phosphorylated retinoblastoma (pRb) was decreased. Overall, these results show that PC4 promotes cell proliferation by activating c-Myc/P21 pathway and accelerate G1/S phase transition in AIPC.

*Depletion of PC4 suppresses EMT-induced metastasis in androgen-independent prostate cancer cells*

Except for cell proliferation, metastasis is the key characteristic of cancer cells. Therefore, we conducted the scratch-wound assay and transwell assay to determine the role of PC4 in AIPC cell migration and invasion. The results showed
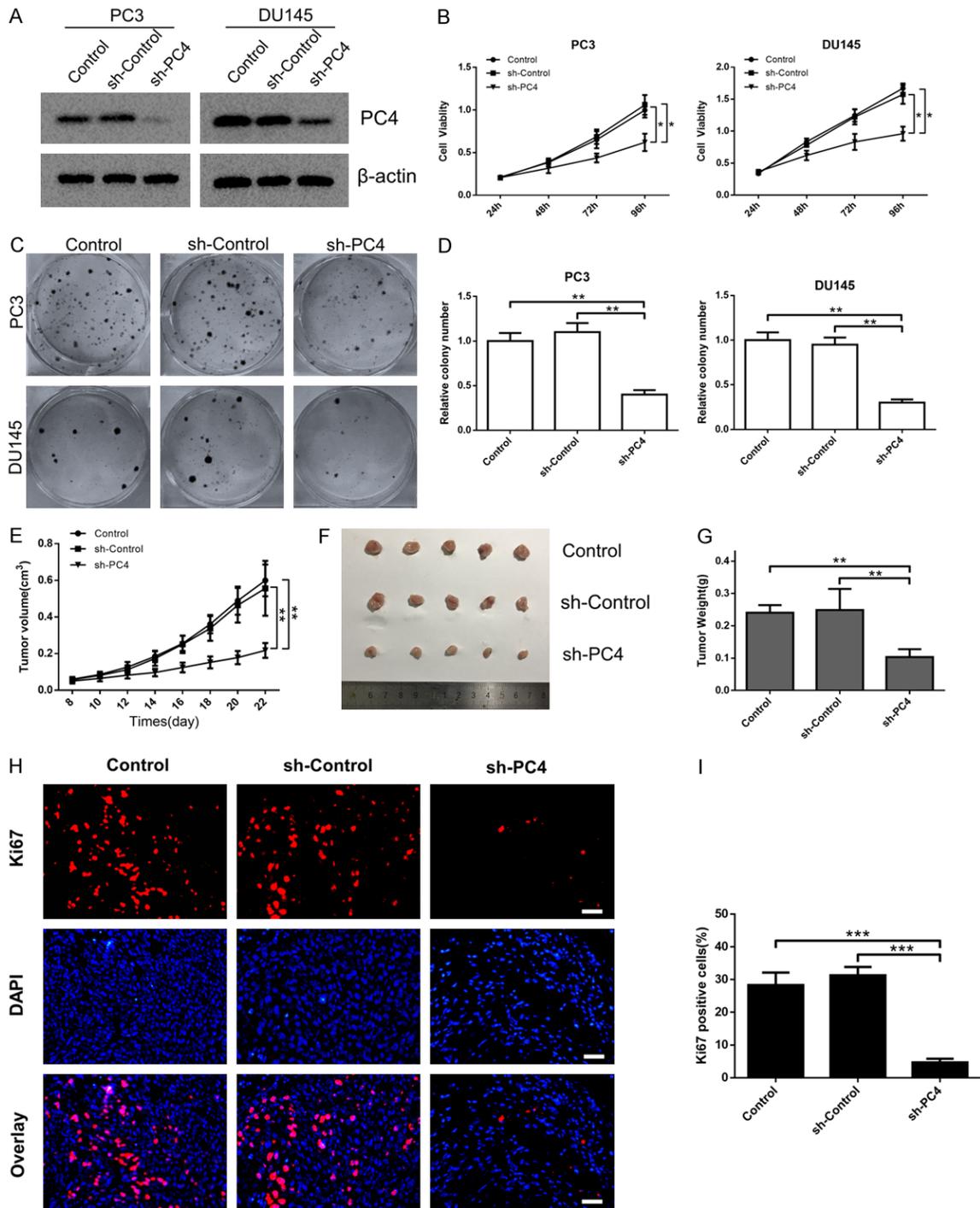
Figure 3. Silencing of PC4 inhibits androgen-independent prostate cancer cell growth both in vitro and in vivo. (A) The stable PC4 knockdown cell lines (PC3 and DU145 cells) were determined by specific shRNA. The PC4 knockout efficiency were examined by western blot. (B) Cell viability in stable PC4 knockdown cell lines (PC3 and DU145 cells) and controls was determined by CCK-8 assay at 24 h, 48 h, 72 h and 96 h. (C) The clone formation assay in stable PC4 knockdown cell lines (PC3 and DU145 cells) and controls. (D) Statistical analysis of the data derived from (C). Experiments were repeated three times independently. (E) The PC3 cell with stable PC4-knockdown was inoculated into athymic male nude mice. Tumor growth curves was measured every 2 days, and the volume was estimated using the following formula: volume = length × width^2/2. (F and G) The dissected xenografts were photographed and weighed at the endpoint. (H and I) Evaluation of proliferation index by Ki67 staining. Scale bar represents 100 µm. All data indicate the mean ± SD. *P<0.05, **P<0.01, ***P<0.001.
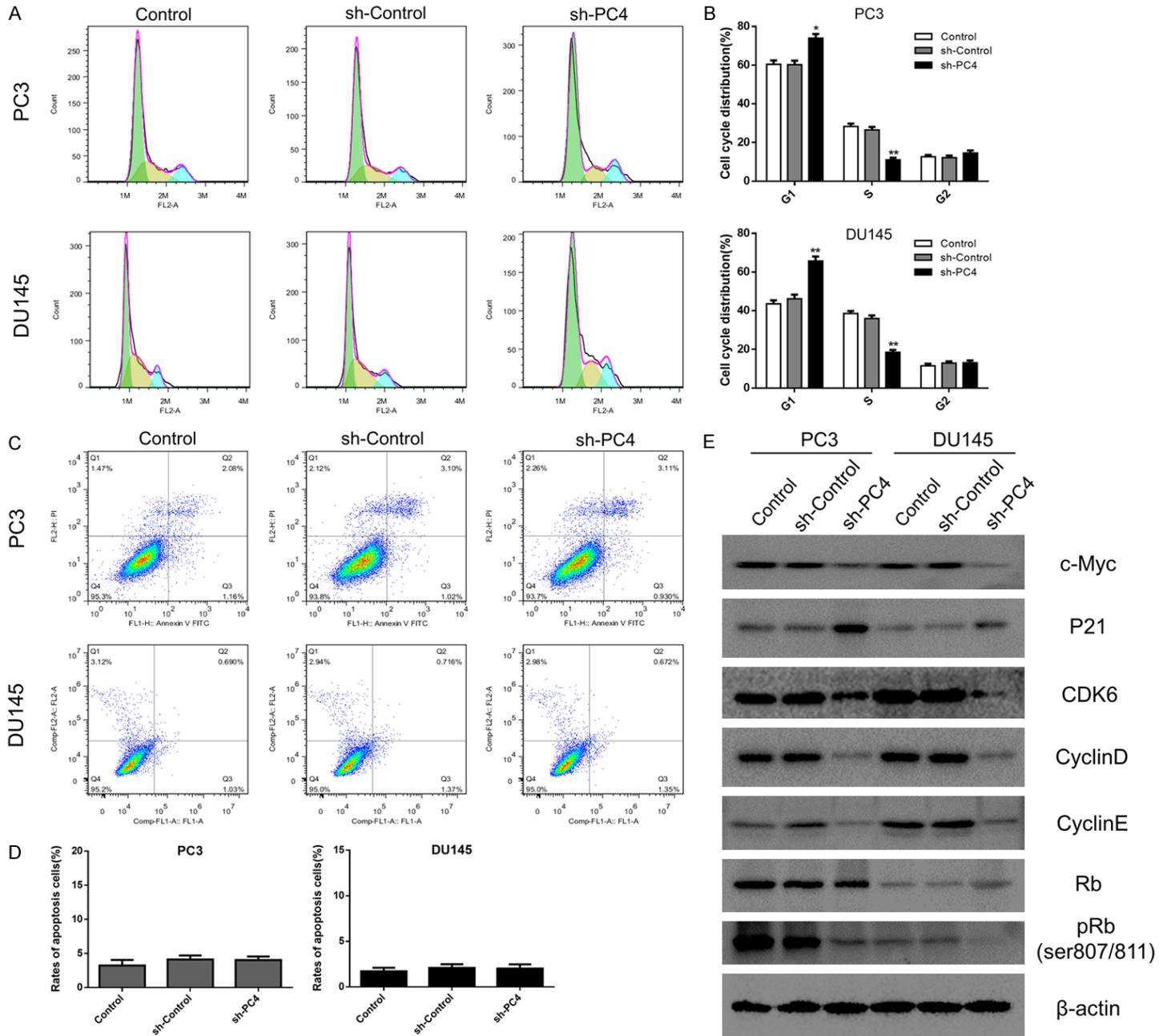
Figure 4. Loss of PC4 induces cell cycle arrest at the G1-to-S phase transition through inhibiting c-Myc/P21 pathway. (A) Cell cycle distribution in stable PC4 knockdown cell lines (PC3 and DU145 cells) and controls was determined by flow cytometry. (B) Statistical analysis of the data derived from (A). Experiments were repeated three times independently. (C) Apoptosis rate in stable PC4 knockdown cell lines (PC3 and DU145 cells) and controls was determined by flow cytometry. (D) Statistical analysis of the data derived from (C). Experiments were repeated three times independently. (E) The protein levels of c-Myc, P21, Cyclin D, Cyclin E, CDK6, Rb and phosphorylated Rb (ser807/811) were determined by Western Blot in stable PC4 knockdown cell lines (PC3 and DU145 cells) and controls. All data indicate the mean ± SD. *P<0.05, **P<0.01.

that depletion of PC4 suppressed cell migration (**Figure 5C** and **5D**) and invasion (**Figure 5A** and **5B**) in both PC3 and DU145 cells. Owing to the critical role of EMT in cancer metastasis [36, 37], we measured the protein levels of EMT markers by Western Blot. As shown in **Figure 5E**, the expression levels of epithelial markers such as E-cadherin were elevated, while the expression levels of mesenchymal markers such as Snail and N-cadherin were reduced in PC4-knockdown cells. Moreover, we established lung metastasis model to evaluate the role of PC4 in cancer metastasis in vivo. PC3 cells with stable PC4-knockdown were tail vein injected into athymic male nude mice. At the endpoint, lung metastatic lesions in PC4-knockdown group were decreased compared with the control groups (Figure S3A and S3B). And hematoxylin-eosin (HE) staining demonstrated that loss of PC4 significantly attenuated the number and size of tumor metastatic foci in lung tissues (**Figure 5F** and **5G**). Therefore, PC4 promotes EMT-mediated metastasis in AIPC.

*PC4 exerts the oncogenic functions through enhancing β-catenin signaling*

Given that c-Myc [38, 39] and EMT-related genes [40, 41] are downstream targets of β-catenin signaling, we hypothesized that loss of PC4 inhibits c-Myc/P21-mediated G1/S phase transition and EMT-induced metastasis through downregulating β-catenin. As shown in **Figure 6A**, immunofluorescent staining revealed that loss of PC4 significantly suppressed the expression of β-catenin in both PC3 and DU145 cells. Western Blot assay (**Figure 6B**) confirmed an obviously decreased of β-catenin in PC4-knockdown cells. To further determine whether β-catenin was required for the oncogenic functions of PC4, the specific plasmid was used to overexpress β-catenin in PC4-knockdown cells (**Figure 6J**). As expected, upregulation of β-catenin rescued the cell cycle arrest in the G1/S transition (**Figure 6C** and **6D**)

and proliferation inhibition (**Figure 6G**) in PC4-knockdown PC3 cells. The inhibitory effects of PC4 knockdown on migration (**Figure 6E** and **6F**) and invasion (**Figure 6H** and **6I**) were also reversed by β-catenin overexpression. Moreover, downregulation of c-Myc, Cyclin D, Cyclin E, N-cadherin and upregulation of P21, E-cadherin in PC4-knockdown cells were all reversed by β-catenin overexpression (**Figure 6J**). Taken together, these results demonstrate that β-catenin is critically involved in the oncogenic functions of PC4 in AIPC.

Activation of β-catenin signaling by PC4 is HIF-1α dependent

Through bioinformatics analysis of GEO database, we found that HIF-1α was positively correlated with high expression of PC4 in cancers. Considering that HIF-1α plays a critical role in cancer progression [42], the qPCR and Western Blot assay were performed to measure the expression levels of HIF-1α in PC4-knockdown AIPC cells. As shown in **Figure 7A** and **7B**, PC4 knockdown markedly suppressed the mRNA and protein level of HIF-1α in both PC3 and DU145 cells. To further determine whether HIF-1α was responsible for the malignant phenotypes of PC4, HIF-1α plasmid was used to overexpress HIF-1α in PC4-knockdown cells. Then, we found that the inhibitory effects of PC4 knockdown on proliferation (**Figure 7D**), migration (**Figure 7E** and **7F**) and invasion (**Figure 7G** and **7H**) were rescued by HIF-1α overexpression. Moreover, upregulation of HIF-1α could rescue the decreased β-catenin in PC4-knockdown cells (**Figure 7I**), indicating that HIF-1α was required for activation of β-catenin signaling by PC4. In addition, overexpression or knockdown of HIF-1α could increase or decrease β-catenin expression (**Figure 7C**), implying that β-catenin was the downstream target of HIF-1α in AIPC cells. Given the above, PC4 promotes proliferation and metastasis of AIPC cells through inducing HIF-1α/β-catenin pathway.
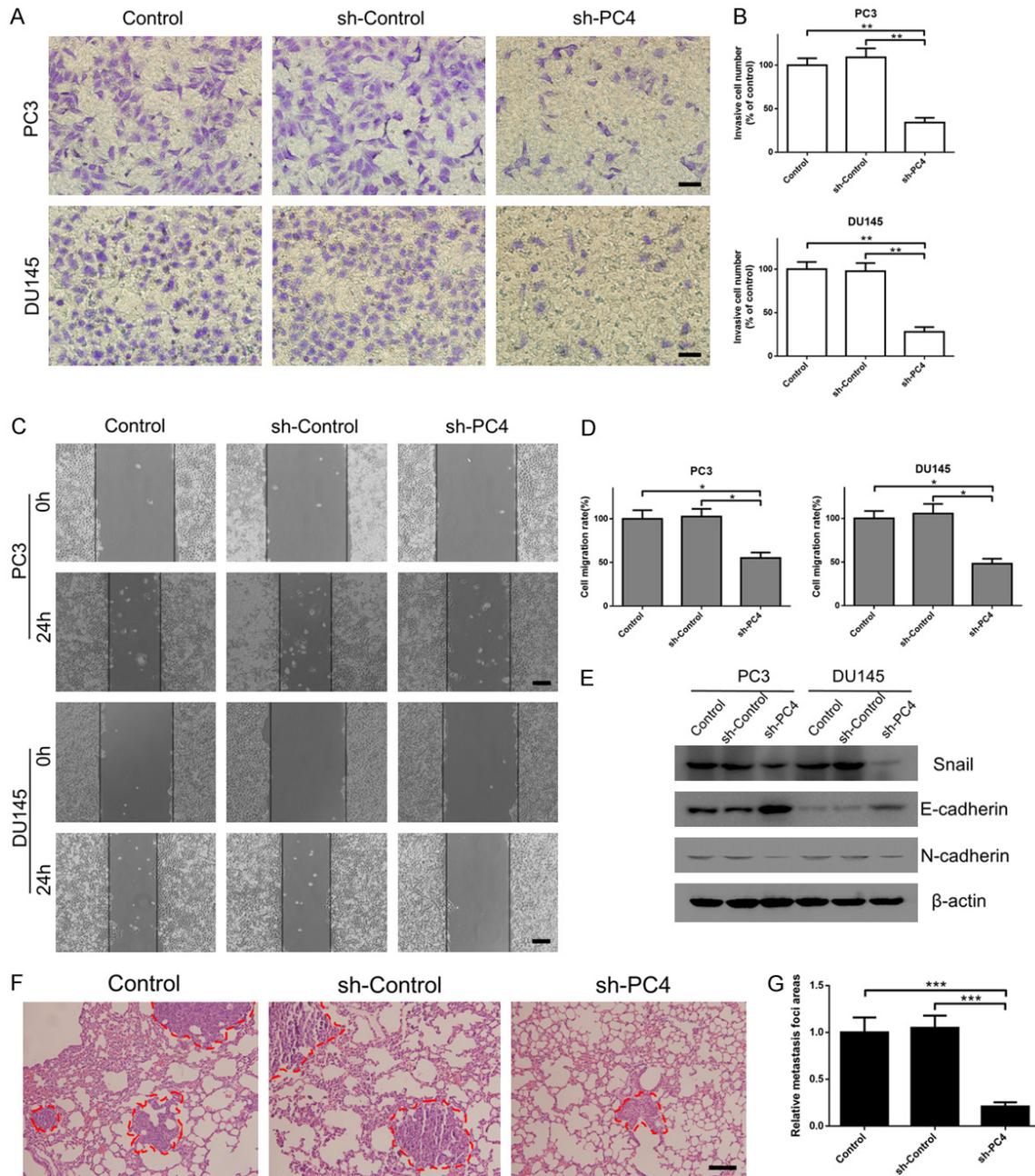
Figure 5. Depletion of PC4 suppresses EMT-induced metastasis in androgen-independent prostate cancer cells. (A) Cell invasive capacity in stable PC4 knockdown cell lines (PC3 and DU145 cells) and controls was determined by transwell assay. Scale bar represents 100 μm. (B) Statistical analysis of the data derived from (A). Experiments were repeated three times independently. (C) Cell migration capacity in stable PC4 knockdown cell lines (PC3 and DU145 cells) and controls was determined by scratch-wound assay. Scale bar represents 200 μm. (D) Statistical analysis of the data derived from (C). Experiments were repeated three times independently. (E) The protein levels of EMT markers (Snail, E-cadherin and N-cadherin) were detected by Western Blot in stable PC4 knockdown cell lines (PC3 and DU145 cells) and controls. (F) Tail vein injection of stable PC4-knockdown and control PC3 cells into athymic male nude mice were used to establish lung metastasis model. Lung tissue was dissected and stained with HE at the endpoint. Scale bar represents 100 μm. (G) Statistical analysis of lung metastatic lesions per mouse in PC4 knockdown group and control groups. All data indicate the mean ± SD. *P<0.05, **P<0.01, ***P<0.001.

Discussion

Owing to the increased recurrence and metastasis and androgen resistance, current strate-gies to treat AIPC are still confronted with great challenges [5, 43]. Thus, there is a serious need to elucidate the underlying molecular mechanisms of AIPC progression and identify
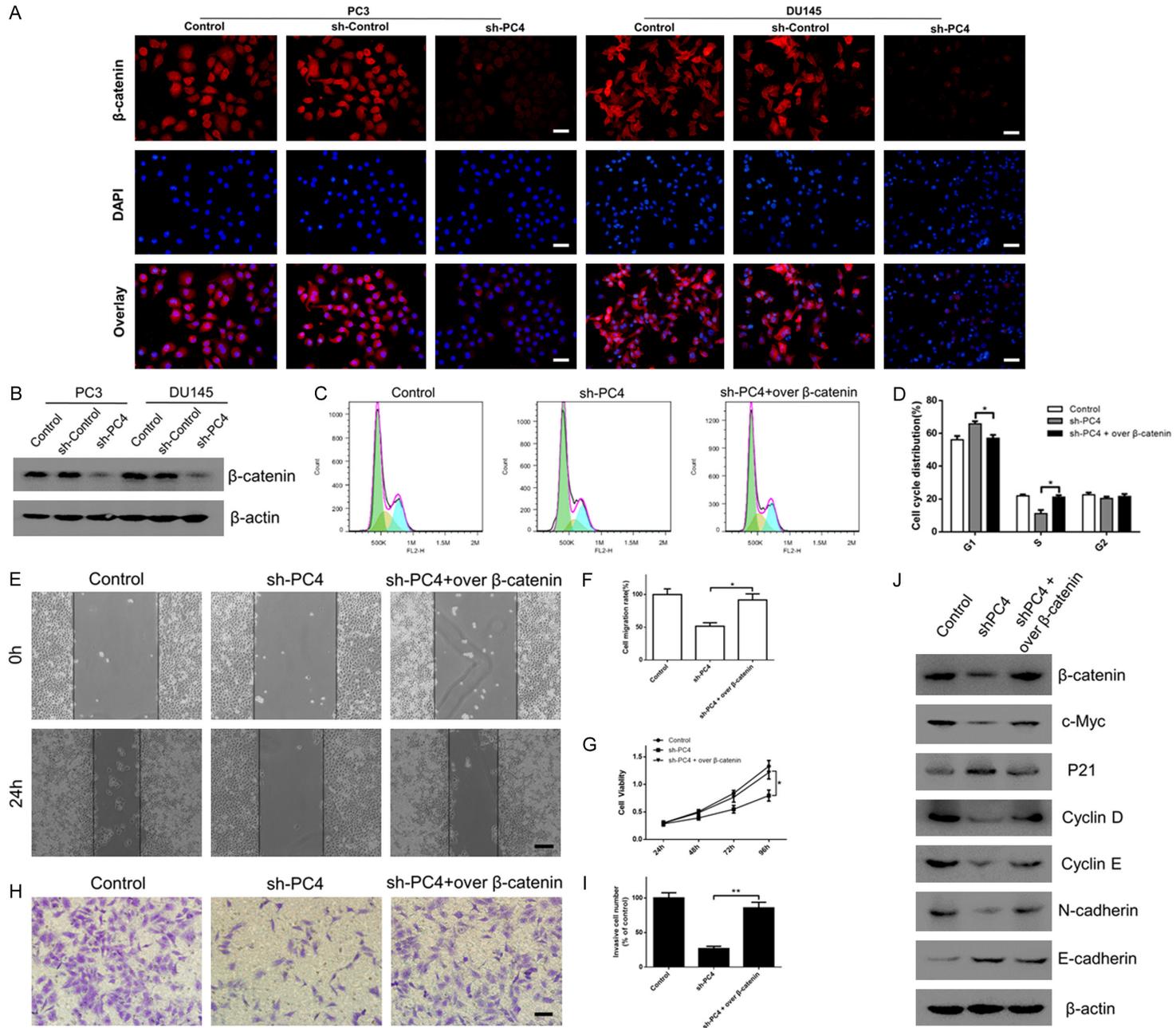
Figure 6. PC4 exerts the oncogenic functions through enhancing β-catenin signaling. (A) Immunofluorescent staining for β-catenin expression in stable PC4 knockdown cell lines (PC3 and DU145 cells) and controls. Scale bar represents 50 μm. (B) Western Blot assay for β-catenin expression in stable PC4 knockdown cell lines (PC3 and DU145 cells) and controls. (C) After overexpression of β-catenin in PC4 knockdown PC3 cells, cell cycle distribution was determined by flow cytometry. (D) Statistical analysis of the data derived from (C). Experiments were repeated three times independently. (E) After overexpression of β-catenin in PC4 knockdown PC3 cells, cell migration capacity was determined by scratch-wound assay. Scale bar represents 200 μm. (F) Statistical analysis of the data derived from (E). Experiments were repeated three times independently. (G) After overexpression of β-catenin in PC4 knockdown PC3 cells, cell viability was determined by CCK-8 assay at 24h, 48h, 72h and 96h. (H) After overexpression of β-catenin in PC4 knockdown PC3 cells, cell invasive capacity was determined by transwell assay. Scale bar represents 100 μm. (I) Statistical analysis of the data derived from (H). Experiments were repeated three times independently. (J) After overexpression of β-catenin in PC4 knockdown PC3 cells, the protein levels of c-Myc, P21, Cyclin D, Cyclin E, Snail and E-cadherin were determined by Western Blot. All data indicate the mean ± SD. *P<0.05, **P<0.01.
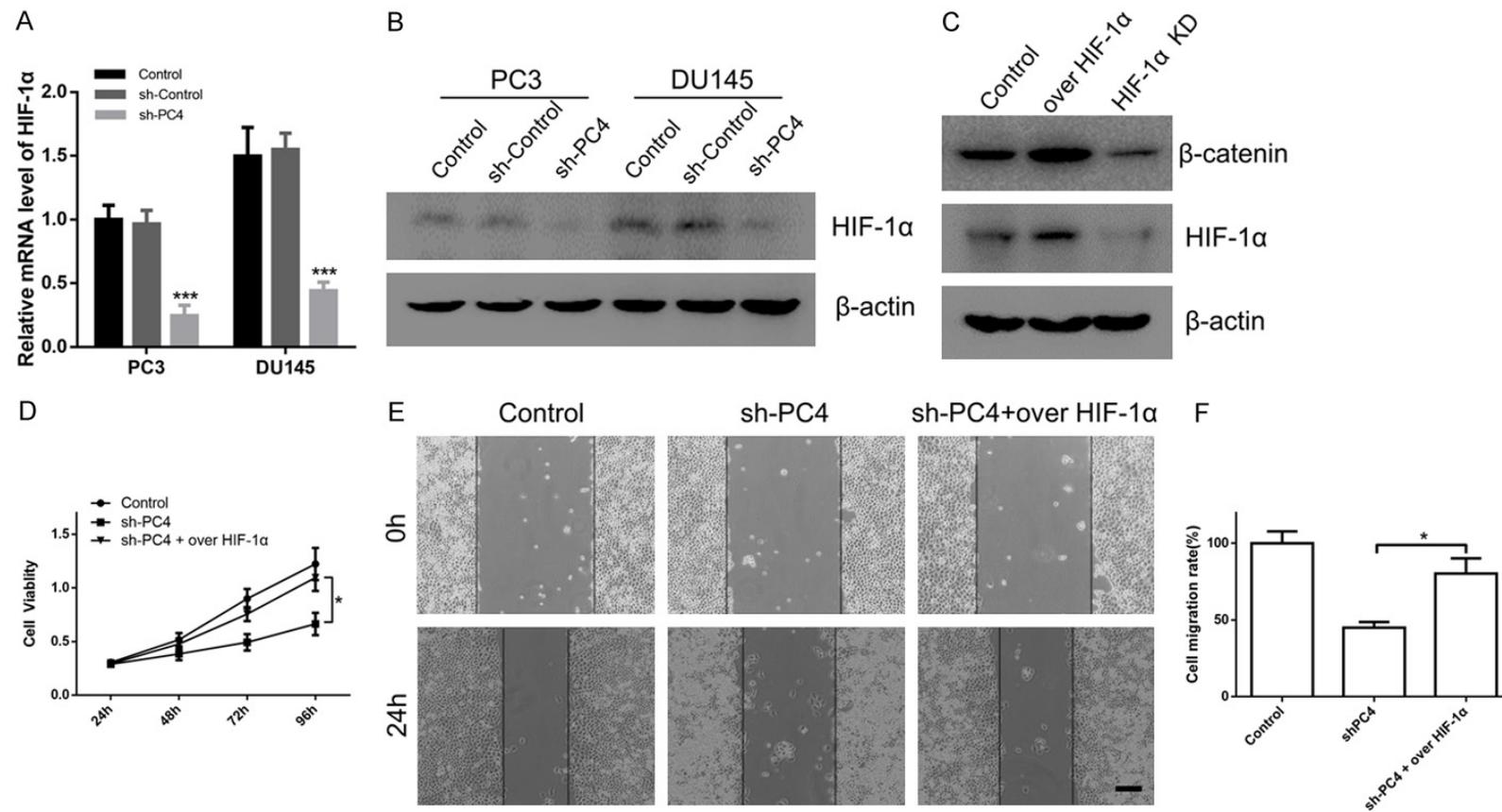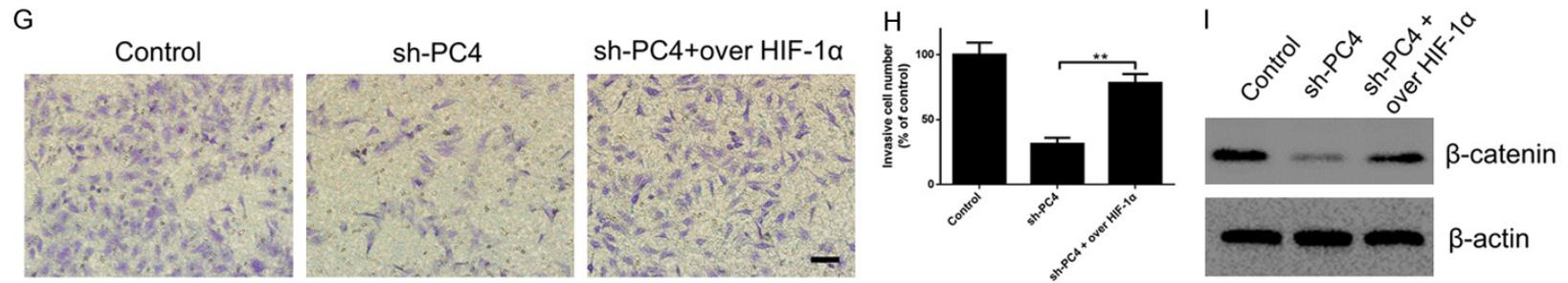
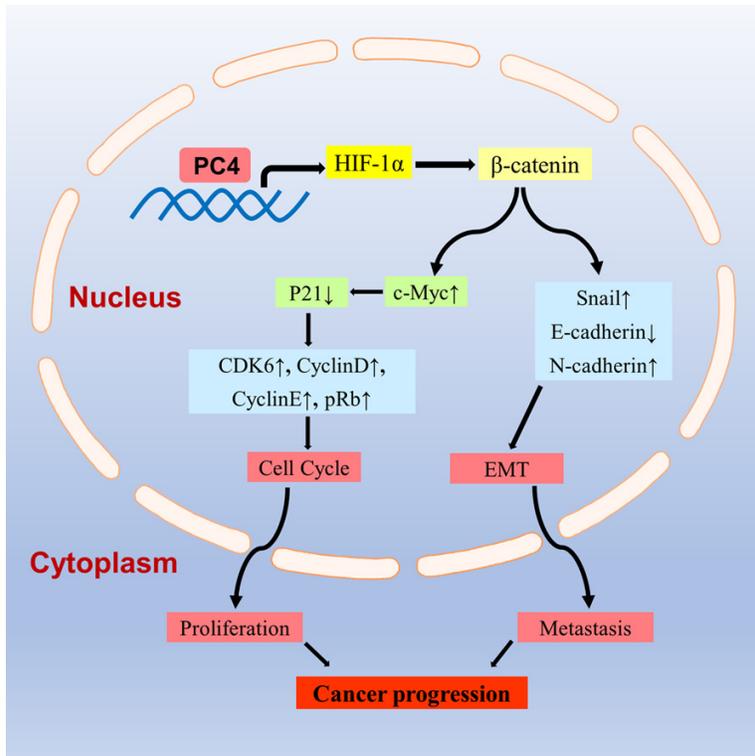**Figure 7.** Activation of β-catenin signaling by PC4 is HIF-1α dependent. (A) The mRNA level of HIF-1α in stable PC4 knockdown cell lines (PC3 and DU145 cells) and controls. (B) The protein level of HIF-1α in stable PC4 knockdown cell lines (PC3 and DU145 cells) and controls. (C) After overexpression or knockdown of HIF-1α in PC3 cells, the protein level of β-catenin was determined by Western Blot. (D) After overexpression of HIF-1α in PC4 knockdown PC3 cells, cell viability was determined by CCK-8 assay at 24 h, 48 h, 72 h and 96 h. (E) After overexpression of HIF-1α in PC4 knockdown PC3 cells, cell migration capacity was determined by scratch-wound assay. Scale bar represents 200 μm. (F) Statistical analysis of the data derived from (E). Experiments were repeated three times independently. (G) After overexpression of HIF-1α in PC4 knockdown PC3 cells, cell invasive capacity was determined by transwell assay. Scale bar represents 100 μm. (H) Statistical analysis of the data derived from (G). Experiments were repeated three times independently. (I) After overexpression of HIF-1α in PC4 knockdown PC3 cells, the protein levels of β-catenin were determined by Western Blot. All data indicate the mean ± SD. *P<0.05, **P<0.01, ***P<0.001.

Figure 8. Schematic illustration for the potential mechanisms of PC4 in AIPC progression. In AIPC, PC4 can promote the expression of HIF-1α and enhance β-catenin signaling. On one hand, β-catenin activates c-Myc and modulates p21 mediated cyclin-dependent kinase-pRb pathway, that accelerates G1/S phase transition to promote cell proliferation in AIPC. On other hand, β-catenin regulates the EMT-related gene and promotes metastasis in AIPC.

in the malignant transformation of normal dermal multipotent fibroblasts, suggesting its importance in cancer progression. Other studies also reveal that inhibition of PC4 radiosensitizes esophageal squmaous cancer [35] and non-small cell lung cancer [50] by transcriptionally suppressing XLF-mediated nonhomologous end joining. Although some studies indicate the potential oncogenic role of PC4 in tumor, how PC4 works in AIPC progression are still unclear. Here, we analysis the clinical data and find that overexpression of PC4 in prostate cancer is closely correlated with differentiation grades and metastasis of patients. The Kaplan-meier analysis exhibits that PC4 was a predictor of poor prognosis for prostate cancer. Compared with ADPC cells, PC4 is significantly upregulated in AIPC cells. To our knowledge, AIPC cells have a more aggressive and invasive phenotype. These findings prompt us to further investigate the functional significance of increased PC4 expression in AIPC. Then, in vivo and in vitro studies exhibit that loss of PC4 evidently suppresses AIPC growth and metastasis, implying its importance as a potential therapeutic target.

novel therapeutic targets to improve AIPC patients' outcomes. Here, we find a novel oncogene, PC4, that is significantly upregulated in AIPC and plays a crucial role in AIPC development and progression through HIF-1α/β-catenin pathway.

Originally isolated from the "upstream stimulatory activity" (USA) of HeLa cell nuclear extracts, PC4 is a multifunctional transcriptional cofactor [20, 21]. By interaction with distinct domains of transcription activators such as AP-2α, NF-κB, Sp1, SMYD3, BRCA1, GAL4 and VP16, PC4 facilitates assembly of the preinitiation complex through bridging between activators and the general transcriptional machinery [44-47]. As a DNA-binding protein, PC4 is also involved in DNA replication, DNA repair and chromatin organization [23, 48, 49]. In PC4 knockout mice, loss of PC4 led to gastrulation arrest in early embryos, highlighting its essential role in embryogenesis. Our previous study shows that upregulation of PC4 is involved

HIF-1α is a key regulator of cellular response to hypoxia. Due to the commonness of hypoxia in solid tumors, HIF-1α is found to be upregulated in various cancer types including prostate cancer [9-11]. As an important transcription factor, HIF-1α is involved in various cellular processes including cell metabolism, growth, differentiation and angiogenesis [8, 18]. In this study, for the first time, we demonstrate that PC4 exertes its oncogenic functions in AIPC by promoting the expression of HIF-1α and activating β-catenin signaling. By the model of brain specific PC4-knockout mice, recently study also found that loss of PC4 could increase the sensitivity to hypoxia in neurons and decrease

the expression of VEGF-A, a key downstream target gene of HIF-1α [51]. To our knowledge, HIF-1α can directly binds to the promoters of the Lef-1 and TCF-1 genes to enhance β-catenin transcription [52, 53]. As a fundamental pathway, Wnt/β-catenin signaling is widely involved in various cellular processes. When aberrantly activated, β-catenin accumulates in the cytoplasm and translocates into the nucleus to promote transcription of target genes, such as c-Myc, Cyclin D1 and EMT-related gene [38, 40]. Then, c-Myc can directly repress the p21 promoter [54] and modulate cyclin-dependent kinase-pRb pathway, that accelerates G1/S phase transition to promote cell proliferation [55, 56]. Taken together, these findings provide novel insights into the signatures and molecular mechanisms of PC4 in AIPC development and progression.

In conclusions, this study provides novel insights into the signatures and molecular mechanisms of PC4 in AIPC progression (**Figure 8**). In AIPC, PC4 can promote the expression of HIF-1α and enhance β-catenin signaling. On one hand, β-catenin activates c-Myc and modulates p21 mediated cyclin-dependent kinase-pRb pathway, that accelerates G1/S phase transition to promote cell proliferation in AIPC. On other hand, β-catenin regulates the EMT-related gene and promotes metastasis in AIPC. Combination with the diagnostic and prognostic value in prostate cancer patients, PC4 may be a promising therapeutic target for AIPC.

Acknowledgements

Disclosure of conflict of interest

None.

Address correspondence to: Chunmeng Shi, Institute of Rocket Force Medicine, State Key Laboratory of Trauma, Burns and Combined Injury, Third Military Medical University, Chongqing 400038, China. E-mail: shicm@sina.com; Weibing Li, Department of Urology and Nephrology, The Third Affiliated Hospital of Chongqing Medical University, Chongqing 401120, China. E-mail: liweibing63@hospital.cqmu.edu.cn

References

[1] Bray F, Ferlay J, Soerjomataram I, Siegel RL, Torre LA and Jemal A. Global cancer statistics 2018: GLOBOCAN estimates of incidence and mortality worldwide for 36 cancers in 185 countries. CA Cancer J Clin 2018; 68: 394-424.

[2] Chen W, Zheng R, Baade PD, Zhang S, Zeng H, Bray F, Jemal A, Yu XQ and He J. Cancer statistics in China, 2015. CA Cancer J Clin 2016; 66: 115-132.

[3] Sartor O. Androgen deprivation therapy in prostate cancer: new findings and questions for the future. Lancet Oncol 2019; 20: 176-177.

[4] Miyamoto H, Messing EM and Chang C. Androgen deprivation therapy for prostate cancer: current status and future prospects. Prostate 2004; 61: 332-353.

[5] Feldman BJ and Feldman D. The development of androgen-independent prostate cancer. Nat Rev Cancer 2001; 1: 34-45.

[6] Lee CH and Kantoff P. Treatment of metastatic prostate cancer in 2018. JAMA Oncol 2018; [Epub ahead of print].

[7] Cully M. Anticancer drugs: cutting down on prostate cancer metastases. Nat Rev Drug Discov 2018; 18: 17.

[8] Vaupel P and Mayer A. Hypoxia in cancer: significance and impact on clinical outcome. Cancer Metastasis Rev 2007; 26: 225-239.

[9] Choudhry H and Harris AL. Advances in hypoxia-inducible factor biology. Cell Metab 2018; 27: 281-298.

[10] Denko NC. Hypoxia, HIF1 and glucose metabolism in the solid tumour. Nat Rev Cancer 2008; 8: 705-713.

[11] Bhandari V, Hoey C, Liu LY, Lalonde E, Ray J, Livingstone J, Lesurf R, Shiah YJ, Vujcic T, Huang X, Espiritu SMG, Heisler LE, Yousif F, Huang V, Yamaguchi TN, Yao CQ, Sabelnykova VY, Fraser M, Chua MLK, van der Kwast T, Liu SK, Boutros PC and Bristow RG. Molecular landmarks of tumor hypoxia across cancer types. Nat Genet 2019; 51: 308-318.

[12] Strzyz P. Cancer biology: hypoxia as an off switch for gene expression. Nat Rev Mol Cell Biol 2016; 17: 610.

[13] Pipinikas CP, Carter ND, Corbishley CM and Fenske CD. HIF-1alpha mRNA gene expression levels in improved diagnosis of early stages of prostate cancer. Biomarkers 2008; 13: 680-691.

[14] Zhong H, Agani F, Baccala AA, Laughner E, Rioseco-Camacho N, Isaacs WB, Simons JW and Semenza GL. Increased expression of hypoxia inducible factor-1alpha in rat and human prostate cancer. Cancer Res 1998; 58: 5280-5284.

[15] Palayoor ST, Mitchell JB, Cerna D, Degraff W, John-Aryankalayil M and Coleman CN. PX-478, an inhibitor of hypoxia-inducible factor-1alpha, enhances radiosensitivity of prostate carcinoma cells. Int J Cancer 2008; 123: 2430-2437.

[16] Rey S, Schito L, Koritzinsky M and Wouters BG. Molecular targeting of hypoxia in radiotherapy. Adv Drug Deliv Rev 2017; 109: 45-62.

[17] Milosevic M, Warde P, Menard C, Chung P, Toi A, Ishkanian A, McLean M, Pintilie M, Sykes J, Gospodarowicz M, Catton C, Hill RP and Bristow R. Tumor hypoxia predicts biochemical failure following radiotherapy for clinically localized prostate cancer. Clin Cancer Res 2012; 18: 2108-2114.

[18] Lawrence YR and Dicker AP. Hypoxia in prostate cancer: observation to intervention. Lancet Oncol 2008; 9: 308-309.

[19] Wigerup C, Pahlman S and Bexell D. Therapeutic targeting of hypoxia and hypoxia-inducible factors in cancer. Pharmacol Ther 2016; 164: 152-169.

[20] Ge H and Roeder RG. Purification, cloning, and characterization of a human coactivator, PC4, that mediates transcriptional activation of class II genes. Cell 1994; 78: 513-523.

[21] Kretzschmar M, Kaiser K, Lottspeich F and Meisterernst M. A novel mediator of class II gene transcription with homology to viral immediate-early transcriptional regulators. Cell 1994; 78: 525-534.

[22] Malik S, Guermah M and Roeder RG. A dynamic model for PC4 coactivator function in RNA polymerase II transcription. Proc Natl Acad Sci U S A 1998; 95: 2192-2197.

[23] Das C, Hizume K, Batta K, Kumar BR, Gadad SS, Ganguly S, Lorain S, Verreault A, Sadhale PP, Takeyasu K and Kundu TK. Transcriptional coactivator PC4, a chromatin-associated protein, induces chromatin condensation. Mol Cell Biol 2006; 26: 8303-8315.

[24] Peng Y, Yang J, Zhang E, Sun H, Wang Q, Wang T, Su Y and Shi C. Human positive coactivator 4 is a potential novel therapeutic target in non-small cell lung cancer. Cancer Gene Ther 2012; 19: 690-696.

[25] Calvo O and Manley JL. The transcriptional coactivator PC4/Sub1 has multiple functions in RNA polymerase II transcription. EMBO J 2005; 24: 1009-1020.

[26] Mortusewicz O, Evers B and Helleday T. PC4 promotes genome stability and DNA repair through binding of ssDNA at DNA damage sites. Oncogene 2016; 35: 761-770.

[27] Chakravarthi BV, Goswami MT, Pathi SS, Robinson AD, Cieslik M, Chandrashekar DS, Agarwal S, Siddiqui J, Daignault S, Carskadon SL, Jing X, Chinnaiyan AM, Kunju LP, Palanisamy N and Varambally S. MicroRNA-101 regulated transcriptional modulator SUB1 plays a role in prostate cancer. Oncogene 2016; 35: 6330-6340.

[28] Lopez CR, Singh S, Hambarde S, Griffin WC, Gao J, Chib S, Yu Y, Ira G, Raney KD and Kim N. Yeast Sub1 and human PC4 are G-quadruplex binding proteins that suppress genome instability at co-transcriptionally formed G4 DNA. Nucleic Acids Res 2017; 45: 5850-5862.

[29] Garavis M, Gonzalez-Polo N, Allepuz-Fuster P, Louro JA, Fernandez-Tornero C and Calvo O. Sub1 contacts the RNA polymerase II stalk to modulate mRNA synthesis. Nucleic Acids Res 2017; 45: 2458-2471.

[30] Du Z, Luo Q, Yang L, Bing T, Li X, Guo W, Wu K, Zhao Y, Xiong S, Shangguan D and Wang F. Mass spectrometric proteomics reveals that nuclear protein positive cofactor PC4 selectively binds to cross-linked DNA by a trans-platinum anticancer complex. J Am Chem Soc 2014; 136: 2948-2951.

[31] Gao J, Zybailov BL, Byrd AK, Griffin WC, Chib S, Mackintosh SG, Tackett AJ and Raney KD. Yeast transcription co-activator Sub1 and its human homolog PC4 preferentially bind to G-quadruplex DNA. Chem Commun (Camb) 2015; 51: 7242-7244.

[32] Shi C, Mai Y, Zhu Y, Cheng T and Su Y. Spontaneous transformation of a clonal population of dermis-derived multipotent cells in culture. In Vitro Cell Dev Biol Anim 2007; 43: 290-296.

[33] Chen L, Du C, Wang L, Yang C, Zhang JR, Li N, Li Y, Xie XD and Gao GD. Human positive co-activator 4 (PC4) is involved in the progression and prognosis of astrocytoma. J Neurol Sci 2014; 346: 293-298.

[34] Tao S, Yu J, Xu Y, Deng B, Sun T, Hu P, Wei Z, Zhang J, Wang R, Shi C and Tan Q. PC4 induces lymphangiogenesis dependent VEGF-C/VEGF-D/VEGFR-3 axis activation in lung adenocarcinoma. Am J Cancer Res 2015; 5: 1878-1889.

[35] Qian D, Zhang B, Zeng XL, Le Blanc JM, Guo YH, Xue C, Jiang C, Wang HH, Zhao TS, Meng MB, Zhao LJ, Hao JH, Wang P, Xie D, Lu B and Yuan ZY. Inhibition of human positive cofactor 4 radiosensitizes human esophageal squmaous cell carcinoma cells by suppressing XLF-mediated nonhomologous end joining. Cell Death Dis 2014; 5: e1461.

[36] Lo UG, Lee CF, Lee MS and Hsieh JT. The role and mechanism of epithelial-to-mesenchymal transition in prostate cancer progression. Int J Mol Sci 2017; 18.

[37] Li P, Yang R and Gao WQ. Contributions of epithelial-mesenchymal transition and cancer stem cells to the development of castration resistance of prostate cancer. Mol Cancer 2014; 13: 55.

[38] Noubissi FK, Elcheva I, Bhatia N, Shakoori A, Ougolkov A, Liu J, Minamoto T, Ross J, Fuchs SY and Spiegelman VS. CRD-BP mediates stabilization of betaTrCP1 and c-myc mRNA in response to beta-catenin signalling. Nature 2006; 441: 898-901.

[39] Cairo S, Armengol C, De Reynies A, Wei Y, Thomas E, Renard CA, Goga A, Balakrishnan A, Semeraro M, Gresh L, Pontoglio M, Strick-Marchand H, Levillayer F, Nouet Y, Rickman D, Gauthier F, Branchereau S, Brugieres L, Laithier V, Bouvier R, Boman F, Basso G, Michiels JF, Hofman P, Arbez-Gindre F, Jouan H, Rousselet-Chapeau MC, Berrebi D, Marcellin L, Plenat F, Zachar D, Joubert M, Selves J, Pasquier D, Bioulac-Sage P, Grotzer M, Childs M, Fabre M and Buendia MA. Hepatic stem-like phenotype and interplay of Wnt/beta-catenin and Myc signaling in aggressive childhood liver cancer. Cancer Cell 2008; 14: 471-484.

[40] Sanchez-Tillo E, de Barrios O, Siles L, Cuatrecasas M, Castells A and Postigo A. beta-catenin/TCF4 complex induces the epithelial-to-mesenchymal transition (EMT)-activator ZEB1 to regulate tumor invasiveness. Proc Natl Acad Sci U S A 2011; 108: 19204-19209.

[41] Santiago L, Daniels G, Wang D, Deng FM and Lee P. Wnt signaling pathway protein LEF1 in cancer, as a biomarker for prognosis and a target for treatment. Am J Cancer Res 2017; 7: 1389-1406.

[42] LaGory EL and Giaccia AJ. The ever-expanding role of HIF in tumour and stromal biology. Nat Cell Biol 2016; 18: 356-365.

[43] Damber JE and Aus G. Prostate cancer. Lancet 2008; 371: 1710-1721.

[44] Kim JM, Kim K, Schmidt T, Punj V, Tucker H, Rice JC, Ulmer TS and An W. Cooperation between SMYD3 and PC4 drives a distinct transcriptional program in cancer cells. Nucleic Acids Res 2015; 43: 8868-8883.

[45] Haile DT and Parvin JD. Activation of transcription in vitro by the BRCA1 carboxyl-terminal domain. J Biol Chem 1999; 274: 2113-2117.

[46] Fukuda A, Nakadai T, Shimada M, Tsukui T, Matsumoto M, Nogi Y, Meisterernst M and Hisatake K. Transcriptional coactivator PC4 stimulates promoter escape and facilitates transcriptional synergy by GAL4-VP16. Mol Cell Biol 2004; 24: 6525-6535.

[47] Zhong L, Wang Y, Kannan P and Tainsky MA. Functional characterization of the interacting domains of the positive coactivator PC4 with the transcription factor AP-2alpha. Gene 2003; 320: 155-164.

[48] Wang JY, Sarker AH, Cooper PK and Volkert MR. The single-strand DNA binding activity of human PC4 prevents mutagenesis and killing by oxidative DNA damage. Mol Cell Biol 2004; 24: 6084-6093.

[49] Garavis M and Calvo O. Sub1/PC4, a multifaceted factor: from transcription to genome stability. Curr Genet 2017; 63: 1023-1035.

[50] Zhang T, Liu X, Chen X, Wang J, Wang Y, Qian D, Pang Q and Wang P. Inhibition of PC4 radiosensitizes non-small cell lung cancer by transcriptionally suppressing XLF. Cancer Med 2018; 7: 1326-1337.

[51] Swaminathan A, Delage H, Chatterjee S, Belgarbi-Dutron L, Cassel R, Martinez N, Cosquer B, Kumari S, Mongelard F, Lannes B, Cassel JC, Boutillier AL, Bouvet P and Kundu TK. Transcriptional coactivator and chromatin protein PC4 is involved in hippocampal neurogenesis and spatial memory extinction. J Biol Chem 2016; 291: 20303-20314.

[52] Mazumdar J, O'Brien WT, Johnson RS, LaManna JC, Chavez JC, Klein PS and Simon MC. O2 regulates stem cells through Wnt/beta-catenin signalling. Nat Cell Biol 2010; 12: 1007-1013.

[53] Braunschweig L, Meyer AK, Wagenfuhr L and Storch A. Oxygen regulates proliferation of neural stem cells through Wnt/beta-catenin signalling. Mol Cell Neurosci 2015; 67: 84-92.

[54] Gartel AL, Ye X, Goufman E, Shianov P, Hay N, Najmabadi F and Tyner AL. Myc represses the p21(WAF1/CIP1) promoter and interacts with Sp1/Sp3. Proc Natl Acad Sci U S A 2001; 98: 4510-4515.

[55] Phan RT, Saito M, Basso K, Niu H and Dalla-Favera R. BCL6 interacts with the transcription factor Miz-1 to suppress the cyclin-dependent kinase inhibitor p21 and cell cycle arrest in germinal center B cells. Nat Immunol 2005; 6: 1054-1060.

[56] Carreira S, Goodall J, Aksan I, La Rocca SA, Galibert MD, Denat L, Larue L and Goding CR. Mitf cooperates with Rb1 and activates p21Cip1 expression to regulate cell cycle progression. Nature 2005; 433: 764-769.

Table S1. List of utilized primer sequence for real-time qPCR

Gene	Forward	Reverse
PC4	TGATTCTGACAGTGAGGTTGAC	TTATCATCTCTGCTGCTGCTG
HIF-1α	GACAGCCTCACCAAACAGAG	CTCAAAGCGACAGATAACACG
β-actin	GGACTTCGAGCAAGAGATGG	AGCACTGTGTTGGCGTACAG
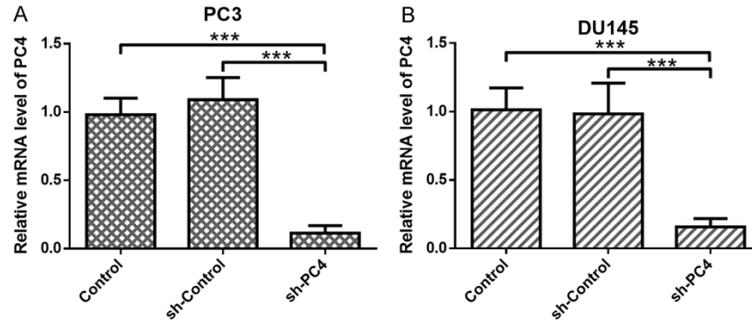
Figure S1. The PC4 knockout efficiency were examined by qPCR in PC3 (A) and DU145 (B) cells. All data indicate the mean ± SD. ***P<0.001.
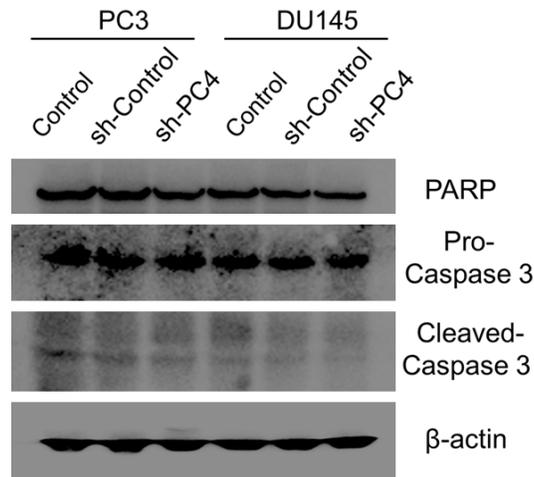
Figure S2. The protein levels of apoptosis markers (PARP, Pro-Caspase 3 and Cleaved-Caspase 3 were determined by Western Blot in stable PC4 knockdown cell lines (PC3 and DU145 cells) and controls.
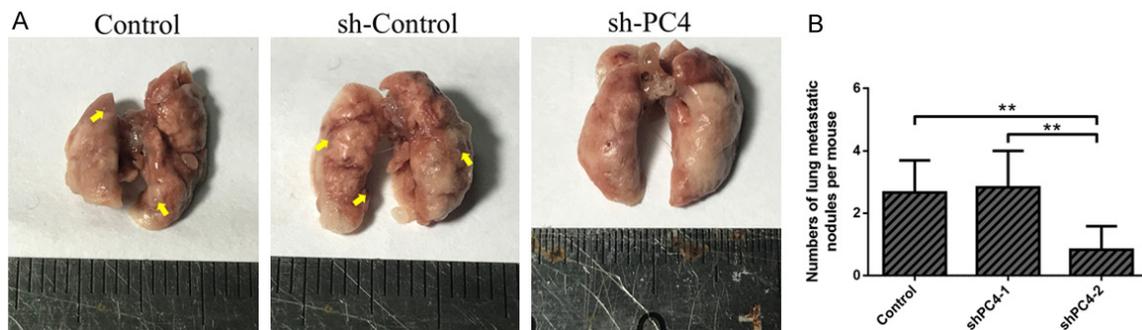
Figure S3. A. Tail vein injection of stable PC4-knockdown and control PC3 cells into athymic male nude mice were used to establish lung metastasis model. Lung tissue was dissected and photographed at the endpoint. B. Statistical analysis of lung metastatic lesions per mouse in PC4 knockdown group and control groups. All data indicate the mean ± SD. **P<0.01.

1